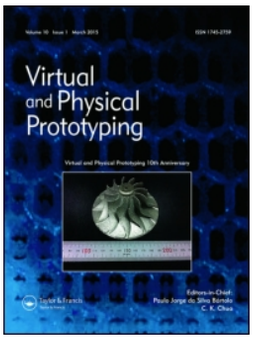

Virtual and Physical Prototyping

ISSN: 1745-2759 (Print) 1745-2767 (Online) Journal homepage: www.tandfonline.com/journals/nvpp20

Extrusion-on-demand methods for high solids loading ceramic paste in freeform extrusion fabrication

Wenbin Li, Amir Ghazanfari, Ming C. Leu & Robert G. Landers

To cite this article: Wenbin Li, Amir Ghazanfari, Ming C. Leu & Robert G. Landers (2017) Extrusion-on-demand methods for high solids loading ceramic paste in freeform extrusion fabrication, Virtual and Physical Prototyping, 12:3, 193-205, DOI: 10.1080/17452759.2017.1312735

To link to this article: https://doi.org/10.1080/17452759.2017.1312735

VIRTUAL AND PHYSICAL PROTOTYPING, 2017
VOL. 12, NO. 3, 193–205
https://doi.org/10.1080/17452759.2017.1312735

Taylor & Francis
Taylor & Francis Group

Extrusion-on-demand methods for high solids loading ceramic paste in freeform extrusion fabrication

Wenbin Li, Amir Ghazanfari, Ming C. Leu and Robert G. Landers

Mechanical and Aerospace Engineering Department, Missouri University of Science and Technology, Rolla, MO, USA

ABSTRACT

Fabrication of highly dense ceramic parts with complex geometries by paste extrusion-based solid freeform fabrication processes requires a precise control of the extrusion start and stop to dispense material on demand, which is often referred to as extrusion-on-demand (EOD). The EOD process for high solids loading pastes is difficult to control due to the paste's non-Newtonian behaviour, compressibility, and inhomogeneity. In this study, three EOD methods based on ram extruder, shutter valve, and auger extruder are investigated for extrusion of high solids loading (>50 vol.%) aqueous ceramic pastes. The extrusion performance characteristics of the three methods in terms of start and stop accuracy, as well as flowrate consistency, are compared and analysed. The results indicate that the auger extruder-based extrusion method has superior EOD performance, and the highest flowrate consistency. Test parts were printed by using these methods and compared to further validate this conclusion.

ARTICLE HISTORY
Received 18 February 2017
Accepted 27 March 2017

KEYWORDS
Additive manufacturing; ceramic; paste; control; extrusion mechanism

1. Introduction

Freeform extrusion fabrication processes such as robocasting (Cesarano *et al*. 1998, Morissette *et al*. 2000, Stuecker *et al*. 2003, Cesarano *et al*. 2005, Miranda *et al*. 2006), contour crafting (Khoshnevis 2004; Kwon and Kim 2007; Khoshnevis *et al*. 2016), fused deposition of ceramics (Agarwala *et al*. 1996, Clancy *et al*. 1997, Lous *et al*. 2000), freeze-form extrusion fabrication (FEF; Huang *et al*. 2006, Mason *et al*. 2006, Leu *et al*. 2011), thermoplastic 3D printing (Scheithauer *et al*. 2015), and ceramic on-demand extrusion (Ghazanfari *et al*. 2016) deposit ceramic extrudate layer-by-layer through material extrusion. Precise control of the deposition flowrate is required to fabricate highly dense parts with complex geometries. Inaccurate extrusion start and stop, as well as fluctuations in the extrudate flowrate, lead to generation of pores in parts, which is a common problem in both filament-based and paste-based freeform extrusion fabrication processes (Agarwala *et al*. 1996, Clancy *et al*. 1997, Huang *et al*. 2006, Scheithauer *et al*. 2015). Throughout the layer-by-layer deposition process, these defects will accumulate and may eventually cause part failure or reduce the strength of the final part, especially for freeform fabrication of brittle ceramic and glass materials (Luo *et al*. 2014, 2015a, 2015b, 2016).

Paste extrusion for freeform extrusion fabrication processes is typically accomplished with a ram extruder, which is a positive placement extruder and consists of a syringe and a plunger. Note that a pneumatic extruder is also used for freeform extrusion fabrication. However, since it controls the extrusion flowrate only by regulating the air pressure instead of piston velocity, its extrusion accuracy is not comparable to a positive displacement extruder (Li and Deng 2004), thus it is not investigated and compared to ram extrusion in this study. Based on ram extrusion, several methods regulating the extrusion force and plunger velocity have been developed for the FEF process. Zhao *et al*. (2010) designed an adaptive controller with a general tracking control law and implemented it to regulate the extrusion force. Deuser *et al*. (2013) developed a hybrid force/velocity controller to regulate both the steady-state extrusion flowrate using a plunger velocity controller and extrusion-on-demand (EOD) using an extrusion force controller. Oakes *et al*. (2009) developed a dwell technique and a look-forward technique to compensate the delay of extrusion start and stop for improving EOD performance. Zomorodi and Landers (2016) developed a hierarchical model-based predictive control algorithm to systematically perform hybrid force–velocity control to extrude paste and draw consistent lines.

The previous efforts to develop ram extruder-based extrusion methods have improved the EOD performance considerably. However, the experimental results still showed that the paste extrusion performance varied

CONTACT Wenbin Li wenbin.li@mst.edu

from batch to batch due to variations in the paste properties. Thus, the control model parameters had to be re-tuned for each batch of paste. Also, for the same batch of paste being extruded using a constant plunger velocity, under-filling and over-filling of material were observed, indicating that the paste flowrate was inconsistent. The paste flowrate inconsistency for a constant plunger velocity is an evidence of the inhomogeneity of the paste properties. Therefore, a more robust EOD method is required.

In this paper, two extrusion mechanisms, that is, shutter valve and auger extruder, which have been utilized in the dispensing industry (Li and Deng 2004), are investigated in comparison with ram extrusion for the freeform extrusion fabrication of ceramics. Extrusion performance characteristics in terms of start and stop accuracy, as well as flowrate consistency, are analysed and compared for these three different EOD methods. Solid parts are also printed using the three EOD methods and their properties are compared. Advantages and drawbacks of these three methods are discussed.

This study focuses on materials that are highly viscous, compressible and inhomogeneous. This type of materials is very common in paste/slurry based freeform extrusion fabrication. Since many researchers are working on freeform extrusion fabrication and are facing the challenge of precise extrusion (e.g. Hong *et al*. 2015, Scheithauer *et al*. 2015, Zomorodi and Landers 2016), it is of prime importance to study the extrusion of this particular type of material. While previous efforts on improving extrusion precision in freeform extrusion fabrication are all based on refining the control model of ram extrusion (Oakes *et al*. 2009, Zhao *et al*. 2010, Deuser *et al*. 2013, Li *et al*. 2013b, Zomorodi and Landers 2016), the present paper introduces a way of improving extrusion precision by comparing different paste extrusion mechanisms and using a proper control scheme for each mechanism. In addition, although the shutter valve and the auger extruder are described as having high dosing accuracy by their suppliers, no rigorous studies investigating their EOD performance and their flowrate consistency, especially for highly viscous, inhomogeneous materials, could be found.

2. Challenges of EOD for high solids loading paste

A schematic along with a photograph of the paste extrusion-based material deposition, is shown in Figure 1(a), where the machine used can be found in a previous article (Zhao, Landers and Leu 2010). Li *et al*. (2013a) modelled the extrusion process by characterizing the ceramic paste viscosity using a modified Herschel–Bulkley model (Herschel and Bulkley 1926). The steady-state relationship between the plunger velocity and the extrusion force was developed based on that viscosity model and the Navier–Stokes equation (Temam 1984). For pastes with different properties, the steady-state extrusion forces for the same plunger velocity were shown to be different. The influence of air presence in the paste was also examined. By regulating the plunger velocity using a general tracking controller (Zhao *et al*. 2010), the plunger velocity reached its steady state very quickly (typically about 1 s). However, the extrusion force responded slowly, reaching a steady-state value in several hundred seconds. Therefore, it took a long time to reach the steady-state extrudate velocity, that is, steady-state paste flowrate. It was concluded that the large settling times of the extrusion force and extrudate velocity were mainly due to the air trapped in the paste (Li *et al*. 2013b). It should be noted that for a high solids loading paste, the degassing process in paste preparation is difficult due to the paste's high viscosity.

The hybrid force–velocity controller developed by Deuser *et al*. (2013) was able to obtain a fast dynamic

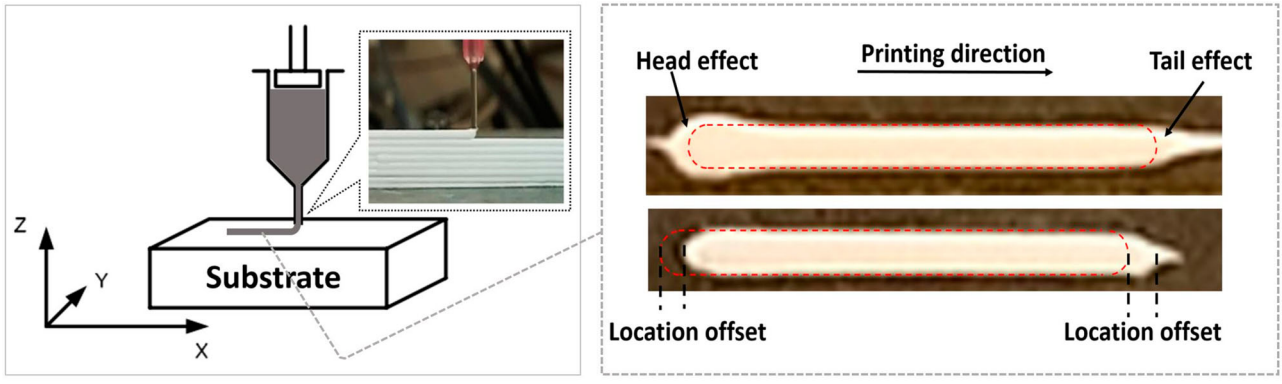

Figure 1. (a) Schematic of paste extrusion-based material deposition and (b) schematic showing print flaws due to inaccurate extrusion start and stop, where the dashed lines indicate desired extrudate shapes and locations.

response of the extrusion force (typically with the settling time between 0.8 and 1.6 s) for start and stop of extrusion using the extrusion force control. During the steady-state extrusion, the controller used the plunger velocity control. The dwell technique and the look-forward technique (Oakes *et al*. 2009) were developed to compensate for the time delay in extrusion start and extrusion stop, respectively. These techniques improved EOD performance considerably. However, the process parameters using a ram extruder must be tuned separately for different batches of paste to achieve high performance since different pastes have different rheological properties. Improper values of extrusion parameters will cause inaccurate extrusion start and stop, resulting in printing flaws. The white regions in Figure 1(b) are actual printed lines, and the dash rounded rectangles represent the desired shapes and locations of printed lines. Excessive material extruded at the start of printing causes a large 'head' of printed line, which will be termed 'head effect'. Ineffective stop of extrusion leaves a 'tail' at the end of printed line, which will be termed 'tail effect'. The head and tail effects are shown in the upper image of Figure 1(b). The lower image in Figure 1(b) shows a printed line not deposited accurately at the desired location due to extrusion time delay, which will be termed 'location offset'.

Moreover, due to the paste's high solids loading, it is difficult to disperse the binder homogeneously during the paste preparation process and thus agglomerates form, causing paste inhomogeneity. Under-filling and over-filling of material were observed under constant velocity printing conditions, indicating inconsistent paste flowrate and providing an evidence for paste inhomogeneity. Since the inhomogeneity of paste properties causes unpredictable disturbances to the ram extrusion process, we consider two other extrusion mechanisms, namely the shutter valve and the auger extruder, in this paper in order to improve EOD performance for the extrusion of high solids loading pastes, which are compressible and inhomogeneous.

3. Different extrusion methods

The paste extrusion process has two distinct phases: steady-state and transient. Steady-state extrusion occurs when a continuous filament is being printed at a constant extrusion rate. Transient extrusion occurs when the flowrate is changing, usually during the start and stop of extrusion. Both phases will be analysed for each of the three extrusion methods. An overall description of the three extrusion mechanisms will be given below first.

3.1. Overall description of the three extrusion mechanisms

The ram extruder mechanism in Figure 2(a) consists of a ram-driven plunger and a syringe. The paste flow is

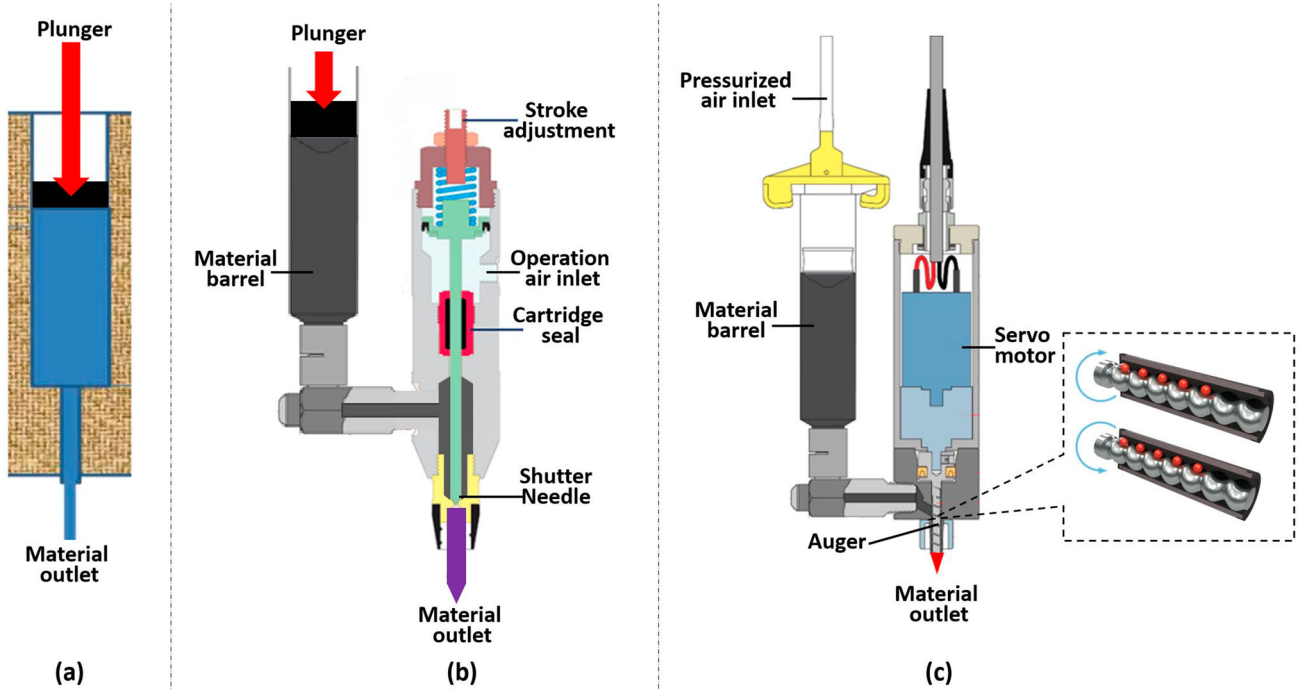

Figure 2. Schematic of three extrusion mechanisms: (a) Ram extruder, (b) shutter valve-based extruder (Nordson Corporation 2010), and (c) Auger extruder (EFD Inc. 2003, ViscoTec Inc. 2014).

regulated by controlling the plunger movement. It starts (or stops) extrusion by generating (or releasing) force on the plunger. Ram extruders are a widely used apparatus for paste extrusion (Benbow and Bridgewater 1993, Li and Deng 2004). A shutter valve extrusion mechanism shown in Figure 2(b) has a plunger and syringe similar to the ram extruder mechanism, except that a shutter needle is added to the flow path as a valve. The shutter needle tip is close to the extrudate outlet. The needle is lifted up or pressed down by an operating force, resulting in the opening and closing of the flow path. The extrusion flowrate is controlled by the plunger velocity or the force applied to the plunger, while the start and stop of extrusion is controlled by the motion of the shutter needle. Shutter valves are widely used in dispensing fluids such as solder paste, conductive epoxy, and adhesive for surface mounting and semiconductor packaging (Li and Deng 2004, Nordson Corporation 2010). The auger extruder mechanism shown in Figure 2(c) also uses a syringe; however, pressure is preloaded to the syringe by compressed air. This preloaded pressure is used for delivering the paste to the auger chamber, rather than for extrusion. Extrusion is achieved by rotating the auger using a servo motor. The flowrate is regulated by controlling the auger's angular velocity. The paste flow is stopped by stopping the auger rotation.

Other extrusion mechanisms that work similarly to auger extruders are collectively referred to as 'progressive cavity pumps', and they are also often referred to as auger pump, screw pump, etc. Auger/screw mechanisms are usually used in fluid dispensing when extra precision or an unlimited feedstock is needed (Li and Deng 2004), such as in micro dosing and injection moulding processes (Bryce 1996). They are also used for powder deposition and metering (Yang and Evans 2007), and have been used in extruding copper paste (Hong *et al*. 2015) and sulphur concrete (Khoshnevis *et al*. 2016) in solid freeform fabrication. However, no rigorous studies investigating the auger extruder's EOD performance and flowrate consistency for inhomogeneous materials could be found. The auger extruder (eco-PEN 300, ViscoTec America Inc., Kennesaw, GA) used in this study consists of a helix metal rotor and an elastomeric stator. Several sealed cavities are formed between the rotor and stator, and they progress down or up when the rotor is turned, as shown in Figure 2(c). Each cavity has a known volume so that the specific volume extruded with each rotation can be determined. This type of auger extruder with a sealing stator is designed for precise micro-dispensing. Auger mechanisms which do not have sealing stators, such as large-scale screw extruders for plastic injection moulding, are not included in the present study.

3.2. Ram extruder-based method

For the ram extruder, the paste flowrate and the start and stop of extrusion are controlled by the plunger velocity and the force exerted by the plunger on the paste material. A general tracking controller has been developed and implemented to regulate the extrusion force and velocity (Deuser *et al*. 2013). Based on this controller, a hybrid extrusion force/velocity control was developed, which includes a plunger velocity control used to ensure a steady extrusion flowrate, and an extrusion force control to regulate the extrusion start and stop. The extrusion force control has a much shorter time constant than the plunger velocity control, and the hybrid control scheme switches from velocity control to force control when extrusion start or stop occurs.

The time constant of extrusion force control, although is shorter than that of the plunger velocity control, causes a delay at the start and stop of extrusion, thus compensation is needed to accurately start and stop extrusion. A schematic of the ram extruder-based method is shown in Figure 3. To start extrusion, the gantry remains stationary, that is, dwelling for a short period of time after the force control is activated (Oakes *et al*. 2009). The amount of this waiting time is called the start dwell time and is denoted τ (refer to Figure 3). To stop extrusion, the force control begins to decrease the extrusion force before the extrusion nozzle reaches the end of the deposition path. The distance between the point where the extrusion force starts to decrease and the desired end of the filament is called the early stop distance and is denoted d (refer to Figure 3).

As discussed in the previous section, extrusion start and stop delays are caused by paste compressibility due to the inevitable existence of air bubbles (Li *et al*. 2013b). The larger the volume of paste being compressed and decompressed during the extrusion start and stop process, the longer the time delay will be. As can be seen in Figure 2(a), the amount of paste being compressed in the ram extruder is the volume of the entire syringe, represented by the blue region in Figure 2(a), and is called the 'operation volume' in this paper. The large operation volume ($\sim$ 55 ml when the syringe in this study is full) of the ram extruder is the main reason of its less than satisfactory EOD performance.

3.3. Shutter valve-based method

Unlike the ram extruder-based method, the start and stop of extrusion in the shutter valve-based method is controlled by the shutter, which opens and closes the flow path. The hybrid extrusion force/velocity control described above is again implemented; however, the

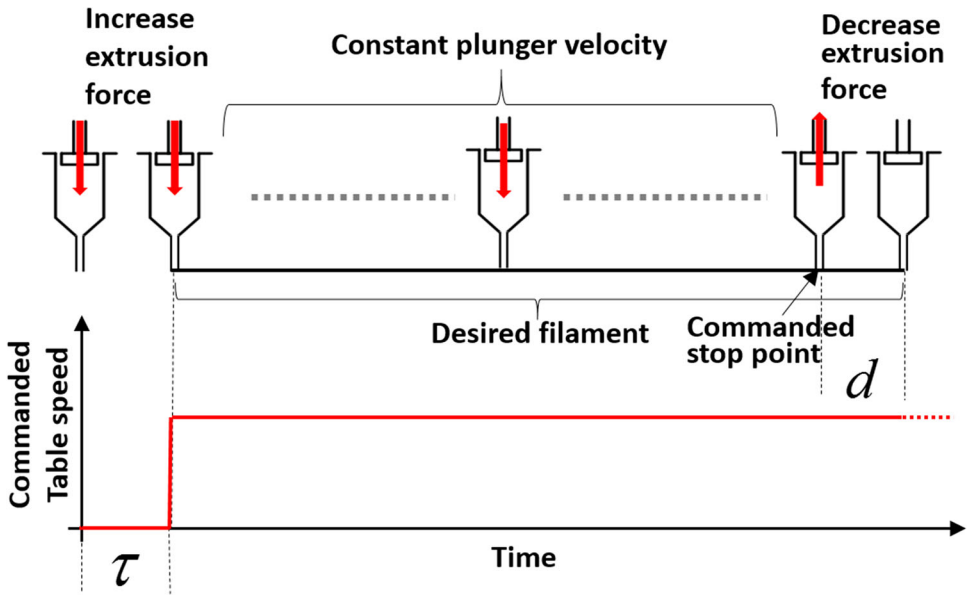

Figure 3. Schematic of ram extruder-based method.

control scheme is adjusted as follows. After the flow path is closed by the shutter, instead of decreasing the force exerted on the plunger, the controller switches from the plunger velocity control mode to the extrusion force control mode to maintain the extrusion force so that the extrusion can be started instantaneously in the next start. It should be noted that during the extrusion start and stop, the paste in the syringe is compressed but is never decompressed; only the paste in the flow path from the shutter to the material outlet will be compressed and decompressed. Then, the controller switches back to the plunger velocity control mode for steady-state extrusion after the flow path is opened in the next operation. For steady-state extrusion, this method is identical to the ram extruder-based method.

By using this method, since the extrusion stop is controlled by directly block the flow path, a very fast stop is expected. On the other hand, the volume of paste being compressed and decompressed during the extrusion start and stop, that is, the operation volume, is the volume of flow path from the shutter to the material outlet, which is represented by the purple region in Figure 2(b). Since the operation volume (~ 0.2 ml for the shutter valve used in this study) is much smaller than that in the ram extruder-based method, a much faster extrusion start is anticipated.

However, the time delay caused by the actuator such as the pneumatic shutter is inevitable and may not be negligible. In order to compensate for any delay of extrusion force and, thus of paste flowrate, the start dwell (τ) and early stop (d) strategies are still used in the shutter valve-based method.

3.4. Auger extruder-based method

When using an auger for paste extrusion, the paste flowrate is proportional to the auger's angular velocity. By maintaining a constant rotation speed of the motor that drives the auger, a constant extrusion flowrate is obtained. The start and stop of extrusion are achieved by turning the motor on and off. The syringe here is only for material storage and delivery, the paste material is only extruded by the auger in the auger chamber. Thus, by using the auger extruder-based method, the operation volume during the extrusion start and stop is the volume from the auger chamber to the material outlet, which is represented by the red region in Figure 2(c). Since the operation volume (~ 0.1 ml for the auger extruder used in this study) is much smaller than that of the ram extruder-based method, a much faster extrusion start and stop is anticipated. Again, in order to compensate for any time delay, the start dwell (τ) and early stop (d) strategies are also used in this method.

For a compressible paste, due to the paste inhomogeneity, the steady-state extrusion force changes during extrusion. For example, the steady-state extrusion force will decrease when a thinner portion of the paste is approaching the nozzle tip and being extruded out; it will increase when a thicker portion or a portion with some large agglomerates is coming out. In other words, the inhomogeneity of the paste properties brings disturbances to the steady-state extrusion process and introduces a transient phase, which is the cause of paste flowrate fluctuation observed when using the ram extruder-based method. An effective

way to alleviate the fluctuation is to have faster responses to these disturbances so that the system reaches its new steady state quickly once a disturbance is present.

A significant difference between the auger extruder-based method and the other two methods is in the steady-state extrusion phase. The ram extruder and shutter valve-based methods have large operation volumes during the steady-state extrusion (~ 50 ml, represented by the blue area in Figure 2(a), and dark grey area plus purple area in Figure 2(b), respectively), resulting in a slow dynamic response of the extrudate velocity and the slow fluctuation of paste flowrate when the corresponding steady-state extrusion force changes. Since the operation volume of the auger valve (represented by red area in Figure 2(c)) is much smaller (~ 0.1 vs. ~50 ml), the dynamic response of extrudate velocity is much faster as compared to the other two methods. Therefore, a better flowrate consistency, that is, less flowrate fluctuation, is expected by using this method compared to using the other two methods.

4. Paste extrusion experiments

In most extrusion-based freeform fabrication processes, the extrusion start and stop accuracy and flowrate consistency are the most important criteria for extrusion performance. Printing dash lines is an effective way to evaluate the extrusion start and stop accuracy, and printing continuous lines is an effective way to evaluate the paste flowrate consistency.

4.1. Paste preparation

The paste used in the extrusion experiments contained Al_2O_3 powder, DARVAN® C (Ammonium polymethacrylate, Vanderbilt Minerals LLC, Gouverneur, NY), Methocel (Methylcellulose, Dow Chemical Company, Pevely, MO) and deionized (DI) water. The Al_2O_3 powder, DARVAN® C and DI water were first mixed and ball-milled for 15 h to form a uniform slurry. DARVAN® C was used as a dispersant to balance the Van der Waals forces between particles. The slurry was then heated up to 70°C and with Methocel dispersed in the slurry agitated by mechanical stirring for 10 min. Then, the slurry was cooled down to room temperature to form the paste. Mechanical stirring was also applied during the cooling down process. Methocel was used as a binder to increase paste viscosity and to assist in forming a stronger green body after drying (Li 2014). Lastly, a vacuum mixer (Model F, Whip Mix Corp., Louisville, KY) was turned on for 10 min to remove air bubbles in the paste.

4.2. Dash line printing

Dash line printing tests were conducted for the three extrusion methods described above. Location offset, tail effect, and head effect in printing dash lines are quantitative measures of the accuracy of extrusion start and stop. Three groups of dash line printing tests with different extrusion conditions listed in Table 1 were conducted. The reference paste flowrate, table speed, and layer thickness were identical for the three extrusion methods in each group. Optimal extrusion parameters for each EOD method including start dwell (τ) and early stop distance (d) were experimentally calibrated for Group 1, that is, for 610 µm diameter nozzle and 60% solids loading paste. The extrusion parameters were calibrated by printing five dash line segments, changing τ by 10 ms and d by 0.1 mm and repeat the printing tries until the best start and stop performance characteristics, that is, having the least head and tail effects and location offset, were achieved. Table 2 lists the values of the obtained τ and d values. Then, the same values of τ and d were applied to Groups 2 and 3 in conducting dash line printing tests. The test results of Group 1 and Group 2 were compared to examine the effects of changing nozzle diameter; the results of Group 1 and Group 3 were compared to examine the effects of changing paste solids loading.

4.3. Continuous line printing

A set of continuous line printing tests were conducted and line width consistency was examined. A special cap was added to the nozzle tip to ensure consistent filament height by restricting the height of the deposited paste. The normal and modified nozzles, as well as their printing schematics, are shown in Figure 4. The filament height (h) was restricted to 150 µm. The reference plunger velocity for the ram extruder was 5 µm/s, which

Table 1. Extrusion conditions of three groups of dash line printing tests.

	Group 1	Group 2	Group 3
Nozzle diameter (µm)	610	406	610
Paste solids loading (%)	60	60	50

Table 2. Calibrated extrusion parameters for 610-µm diameter nozzle and 60% solids loading paste.

Extrusion conditions (extrusion method)	Calibrated extrusion parameters	
	τ (ms)	d (mm)
Ram extruder	450	1.9
Shutter valve	70	0.3
Auger extruder	0	0

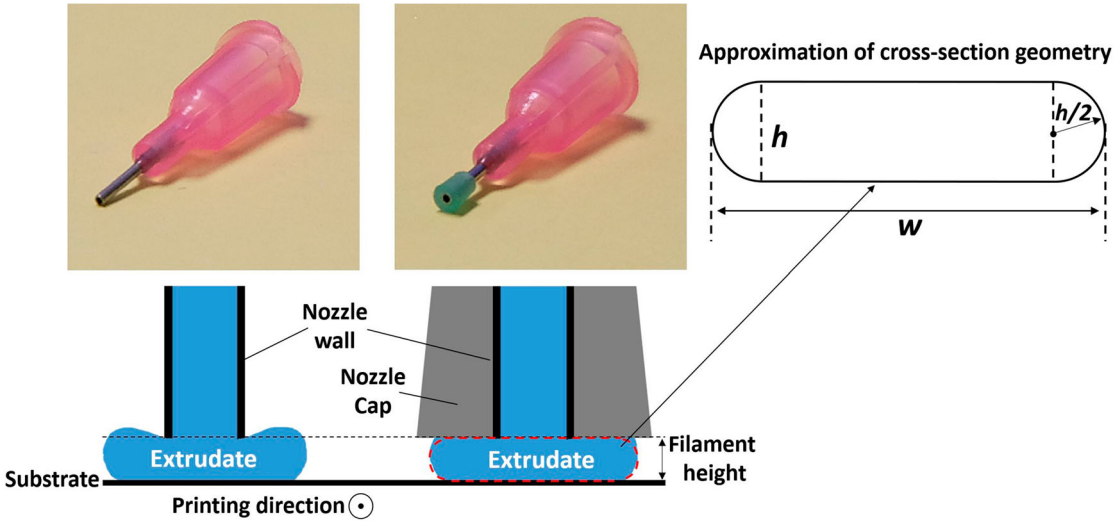

Figure 4. Normal nozzle (left) and nozzle with cap (right) and their printing schematics.

corresponds to a paste flowrate of 0.198 ml/min, and the table speed was set to 660 mm/min, which is a typical speed for this fabrication process. The filament height was set to 150 µm, which is smaller than the typical value of 450 µm, in order to obtain a larger nominal filament width and to reduce the filament width measuring error. By approximating the filament's cross-section geometry as a rectangle rounded at the two ends, as shown in Figure 4, the nominal filament width (w) of 2.02 mm was calculated.

As discussed in the previous section, the ram extruder-based method and the shutter valve-based method are essentially the same for continuous line printing (i.e. steady-state extrusion). Hence, the three extrusion methods were divided into two categories for the continuous line printing tests: the ram extruder/shutter valve-based method and the auger extruder-based method. The shutter valve-based method was chosen to represent the ram extruder/shutter valve category in this experiment. Under these two categories, four groups of dash line printing tests with the experimental conditions listed in Table 3 were conducted. Each group of tests was performed by printing five continuous serpentine lines using the same batch of 60% solids loading paste. Images of the continuous lines were taken and the filament widths at 350 random sampling points were measured by an image processing software (ImageJ, National Institute of Health). The quality of the printed filament was evaluated statistically.

Table 3. Experimental conditions of the four groups of continuous line printing tests.

	Group 1	Group 2	Group 3	Group 4
Nozzle diameter (µm)	610	406	610	406
EOD method	Shutter valve	Shutter valve	Auger extruder	Auger extruder

4.4. Solid part printing

In addition to the above line printing experiments, solid parts were fabricated in order to further examine the extrusion start and stop performance and flowrate consistency for the three EOD methods. Printing solid parts is less forgiving to material under-filling and over-filling compared to printing sparse-build parts such as scaffolds. When a solid part is printed, under-fillings will result in undesired pores, while over-fillings will result in accumulation of extra material and eventually the deposited material will interfere with the nozzle. Since the ram extruder-based method and the shutter valve-based method are essentially the same for continuous printing, only the shutter valve-based method was chosen to compare with the auger extruder-based method in the fabrication of solid parts.

Blocks with dimensions of $30 \times 15 \times 4$ mm^3 were fabricated using the shutter valve and auger extruder-based methods with the same gantry, same batch of paste, and identical process parameters which include paste flowrate: 280 µL/min, raster width: 600 µm, layer thickness: 400 µm, table speed: 21 mm/s, and nozzle diameter: 610 µm. Note that the reference plunger velocity of the shutter valve group was calculated from the reference paste flowrate, and the actual mean extrusion flowrate of the auger extruder-based methods was calibrated to be close to the reference flowrate (280 µL/min) with less than 0.5% error before the experiment. Also, the parts were dried and sintered under the same conditions: 25°C and 75% relative humidity for 20 h to dry the parts,

and 1550°C for 1.5 h to sinter them. The densities of the sintered blocks were measured by Archimedes' method (ASTM International 2014).

5. Results and discussion

5.1. Accuracy of extrusion start and stop

The results of the dash line printing experiments were compared for the three extrusion methods. In Figures 5 and 6, all the dash lines were printed from right to left, and the dashed and solid vertical lines at the two ends represent the desired start and stop points of lines segments, respectively. As shown in Table 2, the values of start dwell time (τ) and early stop distance (d) in the shutter valve and auger extruder-based methods are smaller than those for the ram extruder-based method, indicating a faster start and stop, which validates the anticipation depicted in Sections 3.2 and 3.3. The calibrated start dwell time (τ) and early stop distance (d) for the shutter valve-based method were expected to be zero since the operation volume of shutter valve was negligible comparing to that of the ram extruder (0.2 vs. 55 ml). However, the obtained τ and d for the shutter valve-based method are 70 ms and 0.3 mm, respectively. This non-negligible time delay is due to the pneumatic actuator of the shutter needle. Moreover, by examining Figures 5 and 6, which contain the dash line segments printed by the shutter valve and auger extruder-based methods, we observe sharper tails than those by the ram extruder-based method, indicating more effective extrusion. By further examining Figure 5, the dash line segments printed by the ram extruder method can be seen to have considerably larger location offset when the nozzle diameter changes from 610 (left) to 406 μm (right), indicating the 406 μm diameter nozzle performs worse than the 610-μm diameter nozzle. Figure 6 shows the dash line segments printed by the ram extruder-based method have relatively larger heads when the paste solids loading changes from 60% to 50%, indicating the 50% solids loading paste performs worse than the 60% solids loading paste. In contrast, the line segments printed by the shutter valve and auger extruder-based methods kept consistent accuracy when changing the nozzle diameter and paste solids loading. Finally, the optimal extrusion process parameters for the ram extruder-based method were experimentally calibrated for Groups 2 and 3, and the results are given in Table 4. It can be seen in this table that the values of the optimal extrusion parameters vary considerably with the change of nozzle diameter and paste solids loading.

5.2. Consistency of extrudate flowrate

As discussed in Section 3.3, the ram extruder-based method and the shutter valve-based method are essentially identical for continuous line printing. Hence the continuous line printing tests were conducted using only the shutter valve-based method for both the ram extruder and shutter valve-based methods. For the four groups in Table 3, five 1778 mm serpentine lines were

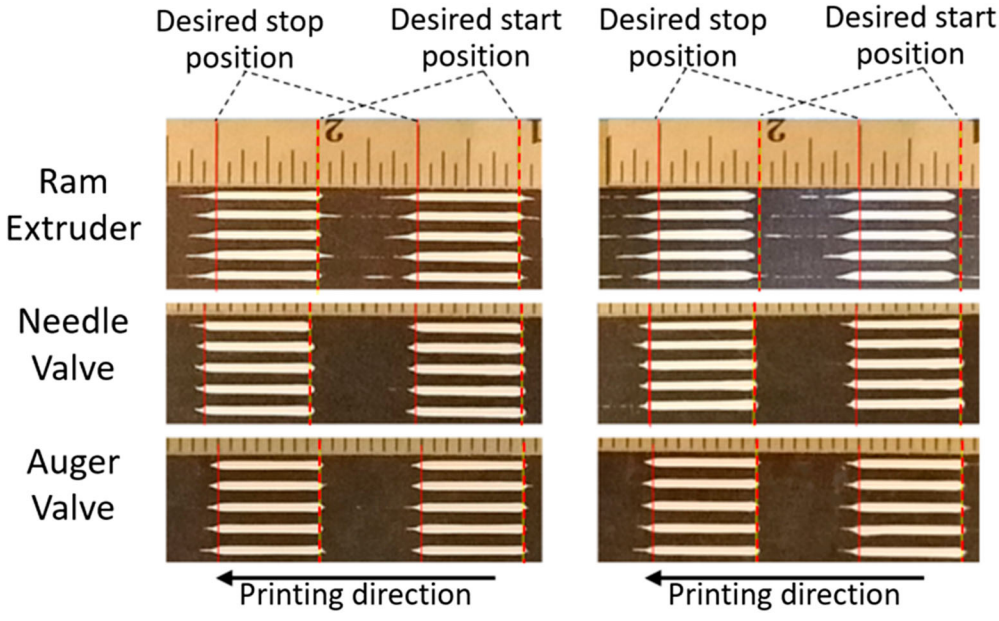

Figure 5. Dash line printing results for 610-μm diameter nozzle (left) and 406-μm diameter nozzle (right), with paste solids loading of 60%.

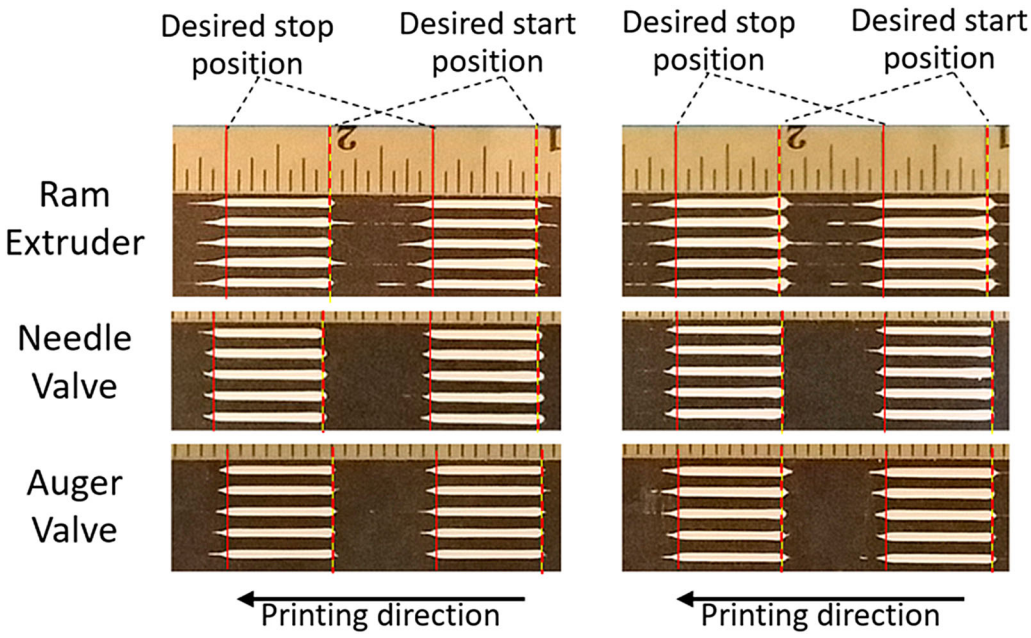

Figure 6. Dash line printing results for 60% solids loading paste (left) and 50% solids loading paste (right), with nozzle diameter of 610 µm.

Table 4. Ram extrusion parameters calibrated for different extrusion conditions.

Group No.	Nozzle diameter (µm)	Paste solids loading (%)	Calibrated extrusion parameters	
			τ(ms)	*d* (mm)
1	610	60	450	1.9
2	406	60	650 (44%)[a]	2.2 (16%)
3	610	50	300 (−33%)	1.3 (−32%)

[a]The numbers in parentheses are the percentage of the parameter variations as compared to the values of group 1, which was previously calibrated and listed in Table 1.

printed for each group. In the images taken, a ruler was placed on the substrate to provide a dimensional scale. Figure 7 shows two images of typical printed serpentine lines using the shutter valve-based method (left) and the auger extruder-based method (right) with a 610-µm diameter nozzle. The substrate consists of a thick polymer tape sticking to a glass plate. As shown in Figure 7, the tape is inside the dashed rectangles. Since the region outside the tape is lower than that inside the tape, measurements were taken only in the areas inside the dashed rectangles to ensure a constant filament height, and also to avoid the transient effects near the corner turns.

A total of four groups of serpentines were measured, with each group containing five serpentine lines. Figure 7 shows two images taken from two of the four groups. A total of 70 measurements of line width were taken for each image, hence a total of 350 measurements were taken for each group. The measured data are plotted in Figure 8, with Figure 8(a) for the two groups using a 610-µm diameter nozzle and Figure 8(b) using

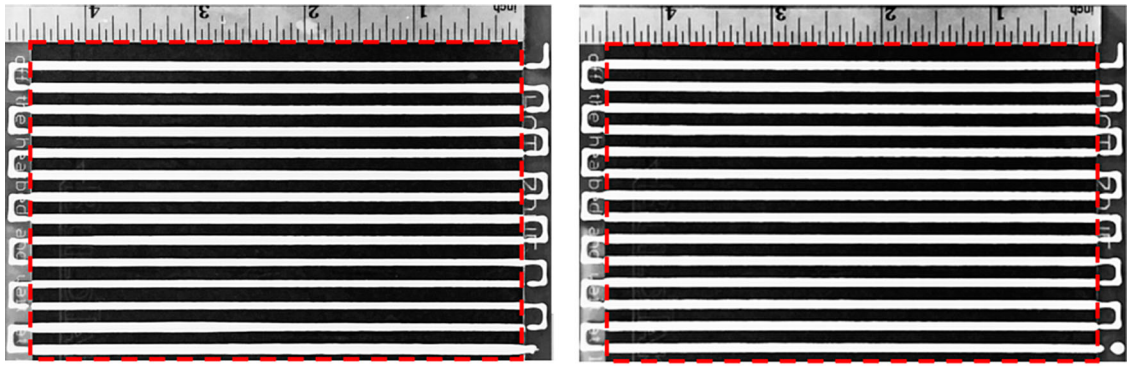

Figure 7. Images of continuous lines printed by shutter valve (left) and auger extruder (right) with 610-µm diameter nozzle. Both serpentine lines were printed from bottom right to top left.

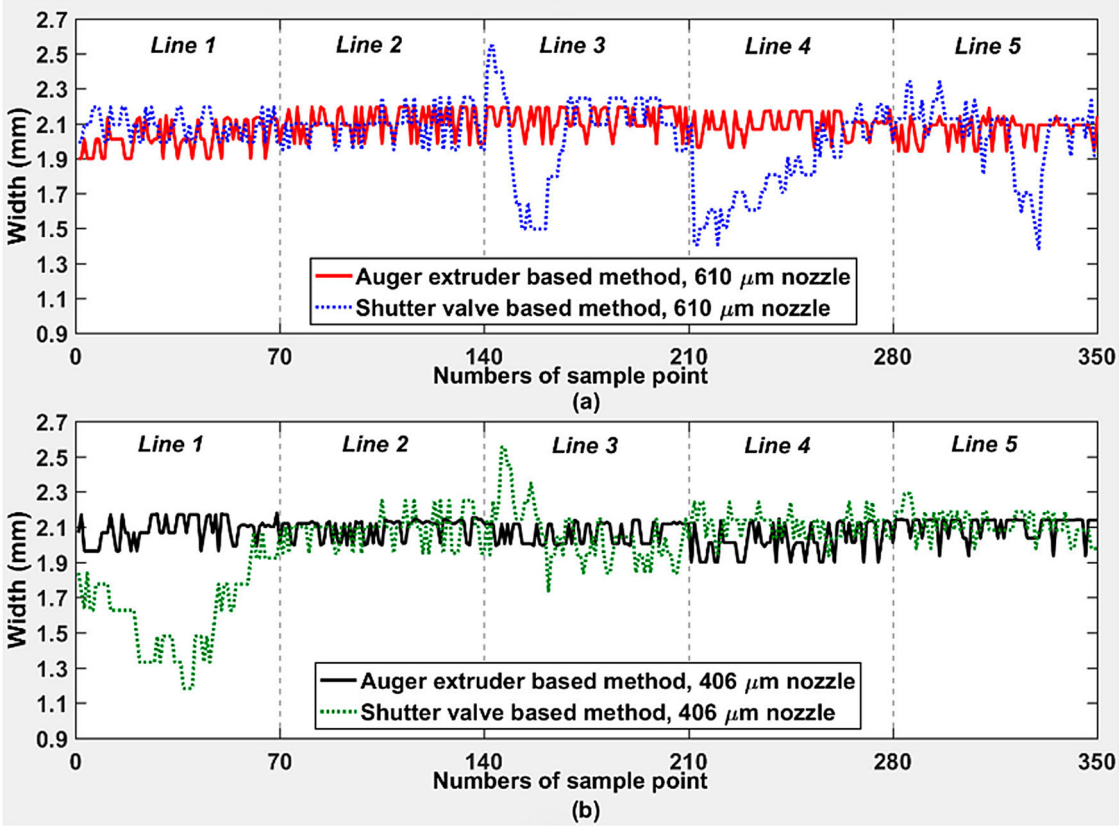

Figure 8. Line widths for continuous line printing experiments using two methods and two nozzle diameters (610 and 406 μm).

a 406-μm diameter nozzle. The line width measured from Figure 7 are plotted in Line 3 of Figure 8(a) using dash and solid curves, respectively, for lines printed using the shutter valve and using the auger extruder. The statistical results obtained from the continuous line printing experiments are given in Table 5. The differences between the mean values of line width and the corresponding nominal values are less than 3% for each group. However, the largest variation for the shutter valve groups is 41.6% vs. 7.9% for the auger extruder groups. The standard deviations of line width for the auger extruder groups are 0.09 and 0.07 mm, for 610 and 406-μm diameter nozzle, respectively, while the standard deviations of line width for the shutter valve groups are 0.22 and 0.24 mm, respectively. It should be noted that the larger (2.9%) mean value errors of the auger extruder groups are due to the lack of self-calibration of the auger extruder controller, that is, there existed an offset between the actual flowrate and the set flowrate appeared on the controller's interface. Also, note that for the solid part printing experiments, self-calibration was done before the experiment.

From Figure 8 and Table 5, we can see the larger fluctuation of paste flowrate in the shutter valve-based method compared with the auger extruder-based method. It can also be seen that for the shutter valve groups, in the printing of one serpentine line, there exist relatively large fluctuations in the line width which occur gradually in some of the sections. This indicates that the transient phases introduced by paste inhomogeneity disturbance have a slow response. A relatively stable flowrate is seen for the auger extruder

Table 5. Results of continuous line printing experiments. Numbers in parentheses are percent difference from the nominal width of 2.02 mm.

	Extrusion condition		Statistical results of printed line width			
Group No.	EOD method	Nozzle diameter (μm)	Mean (mm)	Max. (mm)	Min. (mm)	Standard deviation (mm)
1	Shutter valve	610	2.02 (0.0%)	2.55 (26.2%)	1.38 (−31.7%)	0.22
2	Shutter valve	406	2.00 (−0.9%)	2.55 (26.2%)	1.18 (−41.6%)	0.24
3	Auger extruder	610	2.08 (2.9%)	2.20 (8.9%)	1.90 (−5.9%)	0.09
4	Auger extruder	406	2.08 (2.9%)	2.18 (7.9%)	1.90 (−5.9%)	0.07

groups, which validate the anticipated result as described in Section 3.3, that is, the auger extruder-based method is less sensitive to the inhomogeneity of the compressible paste.

5.3. Relative density of sintered parts

The mean density measured for the blocks printed using the shutter valve-based method was 96.2% of the theoretical density, and that of the blocks printed using the auger value-based method was 98.4% of the theoretical density. Due to the simplicity of the part geometry and its tool path, there were no defects caused by extrusion starts and stops. The higher porosity for printed parts ($30 \times 15 \times 4$ mm^3) using the shutter valve-based method was the result of internal pores caused by the material under-fillings due to variations in the widths of the printed lines. This provides a further evidence that the auger extruder-based extrusion method has better performance in terms of paste flowrate consistency than the shutter valve and ram extruder-based extrusion methods. Three blocks printed using the auger extruder in green state are shown in Figure 9.

5.4. Discussion on extrusion method selection

In addition to the extrusion precision discussed above, another important advantage of the auger extruder-based method is its capability of continuous printing with a large volume of paste. By replacing the system's material barrel (see Figure 2) with a large paste reservoir and feeding the material with a pipe, the auger extruder-based method can potentially print a paste continuously without the limitation of feedstock volume. Nevertheless, one disadvantage of the auger extruder-based method is that the auger and seal rubber are susceptible to wear, especially in printing abrasive materials (Benbow and Bridgewater 1993, ViscoTec Inc. 2014, Khoshnevis *et al*. 2016).

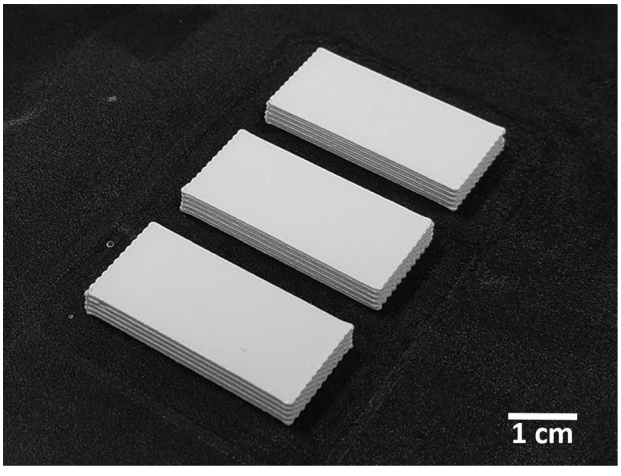

Figure 9. Three solid blocks (green state) printed using an auger extruder for density measurement.

Based on the findings of this study and considering the other advantages and disadvantages of each extrusion method, tentative guidelines for choosing an extrusion mechanism for freeform extrusion fabrication are given below:

- In the cases that compact extruder size, high extrusion start and stop accuracy, great flowrate consistency, and unlimited feedstock volume are required, especially when the material lacks homogeneity, the auger extruder mechanism is suggested. An example is printing pore-free large ceramic parts. For extrusion of abrasive materials, however, the wear of auger will need to be considered.
- In the cases where large extruder size/weight is allowed, and high-precision control of extrusion start and stop for inhomogeneous materials is required, the shutter valve mechanism is suggested as a low-cost option.
- In the cases where the material is highly homogenous or incompressible, or the extrusion precision is not critical, the ram extruder mechanism is suggested due to its low cost and simplicity. Another case suitable for the ram extruder is when the material does not need to be much pressurized, such as in extruding with a large nozzle.

6. Conclusions

Extrusion-on-demand (EOD) methods based on ram extruder, shutter valve, and auger extruder have been presented and investigated for freeform extrusion fabrication of high solids loading ceramic pastes. The accuracy of extrusion start and stop and consistency of paste flowrate were compared for these three methods by performing experiments that print dash and continuous lines. Also, the densities of the sintered ceramics parts were measured and compared for solid blocks printed using the different EOD methods. Advantages and disadvantages of each method were discussed, and tentative guidelines for selecting the extrusion mechanism were given. Conclusions are drawn from the experimental results as follows:

- The shutter valve and auger extruder-based methods exhibit much shorter time delays than the ram extruder-based method for extrusion start and stop.
- The shutter valve and auger extruder-based methods are more robust for accurate control of extrusion start

and stop than the ram extruder-based method. The calibrated control parameters for extrusion start and stop can be kept constant for different batches of paste and different nozzle diameters when using the shutter valve and auger extruder-based methods. However, the ram extruder-based method needs to adjust its control parameters for extrusion start and stop for different paste solids loading and nozzle diameter.

- The auger extruder-based method is more robust for continuous printing than the ram extruder and shutter valve-based methods. For a constant set extrusion rate, the auger extruder-based method has higher consistency in the printed line width than the other two methods.
- The sintered solid ceramic parts printed using the auger extruder-based method have higher density than the part densities obtained using ram extruder and shutter valve-based methods.

Disclosure statement

No potential conflict of interest was reported by the authors.

Funding

This work was supported by the Intelligent Systems Center at the Missouri University of Science and Technology; Department of Energy of the U. S. Department of Energy's Office of Fossil Energy [grant number DE-FE0012272].

References

Agarwala, M.K., *et al.*, 1996. FDC, rapid fabrication of structural components. *American Ceramic Society Bulletin*, 75 (11), 60–66.

ASTM International, 2014. ASTM C373-14a. *Standard test method for water absorption, bulk density, apparent porosity, and apparent specific gravity of fired whiteware products, ceramic tiles, and glass tiles*.

Benbow, J. and Bridgewater, J., 1993. *Paste flow and extrusion*. Oxford: Clarendon Press.

Bryce, D.M., 1996. *Plastic injection molding: manufacturing process fundamentals*. Dearborn, MI: Society of Manufacturing Engineers.

Cesarano, J., Segalman, R., and Calvert, P., 1998. Robocasting provides moldless fabrication from slurry deposition. *Ceramic Industry*, 148 (4), 94.

Cesarano, J., *et al.*, 2005. Customization of load-bearing hydroxyapatite lattice scaffolds. *International Journal of Applied Ceramic Technology*, 2 (3), 212–220.

Clancy, R., *et al.*, 1997. Fused deposition of ceramics: progress towards a robust and controlled process for commercialization. *In*: D. Bourell, J. Beaman, and R. Crawford, eds. *Proceedings of the 8th annual international solid freeform fabrication symposium*. Austin, TX: TMS, 185–194.

Deuser, B.K., *et al.*, 2013. Hybrid extrusion force-velocity control using freeze-form extrusion fabrication for functionally graded material parts. *Journal of Manufacturing Science and Engineering*, 135 (4), 041015-041015-11.

EFD Inc., 2003. *Auger valve dispensing*. Available from: http://www.smtnet.com/library/files/upload/EFD_-_Auger_Valve_Dispensing.pdf [Accessed 17 February 2017].

Ghazanfari, A., *et al.*, 2016. A novel extrusion-based additive manufacturing process for ceramic parts. *In*: D. Bourell, J. Beaman, and R. Crawford, eds. *Proceedings of the 27th annual international solid freeform fabrication symposium*. Austin, TX: TMS, 1509–1529.

Herschel, W. and Bulkley, R., 1926. Measurement of consistency as applied to rubber benzene solutions. *American Society for Testing Materials*, 26 (82), 621–629.

Hong, S., *et al.*, 2015. Fabrication of 3D printed metal structures by use of high-viscosity Cu paste and a screw extruder. *Journal of Electronic Materials*, 44 (3), 836–841.

Huang, T., *et al.*, 2006. Freeze-form extrusion fabrication of ceramic parts. *Virtual and Physical Prototyping*, 1 (2), 93–100.

Khoshnevis, B., 2004. Automated construction by contour crafting-related robotics and information technologies. *Automation in Construction*, 13 (1), 5–19.

Khoshnevis, B., *et al.*, 2016. Construction by contour crafting using sulfur concrete with planetary applications. *Rapid Prototyping Journal*, 22 (5), 848–856.

Kwon, H.K. and Kim, K.S., 2007. Effect of orifice shape in contour crafting with ceramic material: a simulation for extrusion and deposition mechanism. *Advanced Materials Research*, 26–28, 953–956.

Leu, M.C., *et al.*, 2011. Freeze-form extrusion fabrication of composite structures. *In*: D. Bourell, J. Beaman, and R. Crawford, eds. *Proceedings of the 22nd annual international solid freeform fabrication symposium*. Austin, TX: TMS, 111–124.

Li, J., 2014. *An experimental study of fabrication temperature effect on aqueous extrusion freeform fabrication*. Rolla, MO: Missouri University of Science and Technology.

Li, J. and Deng, G., 2004. Technology development and basic theory study of fluid dispensing – a review. *In*: J. Liu and T. Yu, eds. *Proceeding of the sixth IEEE CPMT conference on high density microsystem design and packaging and component failure analysis*. Shanghai: IEEE, 198–205.

Li, M., *et al.*, 2013a. Extrusion process modeling for aqueous-based ceramic pastes – part 1: constitutive model. *Journal of Manufacturing Science and Engineering*, 135 (5), 051008-051008-7.

Li, M., *et al.*, 2013b. Extrusion process modeling for aqueous-based ceramic pastes – part 2: experimental verification. *Journal of Manufacturing Science and Engineering*, 135 (5), 051009-051009-7.

Lous, G.M., *et al.*, 2000. Fabrication of piezoelectric ceramic/polymer composite transducers using fused deposition of ceramics. *Journal of the American Ceramic Society*, 83 (1), 124–128.

Luo, J., Pan, H., and Kinzel, E.C., 2014. Additive manufacturing of glass. *Journal of Manufacturing Science and Engineering*, 136 (6), 061024-061024-6.

Luo, J., *et al.*, 2015a. Solid freeform fabrication of transparent fused quartz using a filament fed process. *In*: D. Bourell, J. Beaman, and R. Crawford, eds. *Proceedings of the 26th annual international solid freeform fabrication symposium*. Austin, TX: TMS, 122–133.

Luo, J., *et al.*, 2015b. Wire-fed additive manufacturing of transparent glass parts. *In*: A.S. Malik and Z. Li (Charlie), eds. *Proceedings of the ASME 2015 international manufacturing science and engineering conference*. Charlotte, NC: ASME, V001T02A108-V001T02A108-5.

Luo, J., *et al.*, 2016. Bubble formation in additive manufacturing of glass. *In*: J.N. Vizgaitis, B.F. Andresen, P.L. Marasco, J.S. Sanghera, and M.P. Snyder, eds. *Proceedings of SPIE 9822, advanced optics for defense application*. Altimore, MD: SPIE, 982214–982216.

Mason, M.S., *et al.*, 2006. Freeform extrusion of high solids loading ceramic slurries, part I: extrusion process modeling. *In*: D. Bourell, J. Beaman, and R. Crawford, eds. *Proceedings of the 17th annual international solid freeform fabrication symposium*. Austin, TX: TMS, 316–328.

Miranda, P., *et al.*, 2006. Sintering and robocasting of β-tricalcium phosphate scaffolds for orthopaedic applications. *Acta Biomaterialia*, 2 (4), 457–466.

Morissette, S.L., *et al.*, 2000. Solid freeform fabrication of aqueous alumina-poly(vinyl alcohol) gelcasting suspensions. *Journal of the American Ceramic Society*, 83 (10), 2409–2416.

Nordson Corporation, 2010. *741 V needle valve system for precise, consistent fluid control*. Available from: http://pdf.directindustry.com/pdf/nordson-efd/741v-needle-valve/35688-657310.html [Accessed 17 February 2017].

Oakes, T., *et al.*, 2009. Development of extrusion-on-demand for ceramic freeze-form extrusion fabrication. *In*: D. Bourell, J. Beaman, and R. Crawford, eds. *Proceedings of the 20th annual international solid freeform fabrication symposium*. Austin, TX: TMS, 206–218.

Scheithauer, U., *et al.*, 2015. Thermoplastic 3D printing – an additive manufacturing method for producing dense ceramics. *International Journal of Applied Ceramic Technology*, 12 (1), 26–31.

Stuecker, J.N., Cesarano, J., and Hirschfeld, D.A., 2003. Control of the viscous behavior of highly concentrated mullite suspensions for robocasting. *Journal of Materials Processing Technology*, 142 (2), 318–325.

Temam, R., 1984. *Navier-stokes equations*. Amsterdam: North-Holland.

ViscoTec Inc., 2014. *Micro dispensing in perfection*. Available from: https://www.viscotec.de/media/preeflow_brochure_2014.pdf [Accessed 17 February 2017].

Yang, S. and Evans, J.R.G., 2007. Metering and dispensing of powder; the quest for new solid freeforming techniques. *Powder Technology*, 178 (1), 56–72.

Zhao, X., Landers, R.G., and Leu, M.C., 2010. Adaptive extrusion force control of freeze-form extrusion fabrication processes. *Journal of Manufacturing Science and Engineering*, 132 (6), 064504-064504-9.

Zomorodi, H., and Landers, R.G., 2016. Extrusion based additive manufacturing using explicit model predictive control. *In*: J. Sun and R. Rajamani, eds. *Proceedings of the 2016 American control conference*. Boston, MA: IEEE, 1747–1752.